



HAL
open science

Biogenic iron preserves structures during fossilization: A hypothesis

Farid Saleh, Allison Daley, Bertrand Lefebvre, Bernard Pittet, Jean-Philippe Perrillat

► To cite this version:

Farid Saleh, Allison Daley, Bertrand Lefebvre, Bernard Pittet, Jean-Philippe Perrillat. Biogenic iron preserves structures during fossilization: A hypothesis. *BioEssays*, 2020, 42 (6), pp.1900243. 10.1002/bies.201900243 . hal-03005026

HAL Id: hal-03005026

<https://hal.science/hal-03005026>

Submitted on 13 Nov 2020

HAL is a multi-disciplinary open access archive for the deposit and dissemination of scientific research documents, whether they are published or not. The documents may come from teaching and research institutions in France or abroad, or from public or private research centers.

L'archive ouverte pluridisciplinaire **HAL**, est destinée au dépôt et à la diffusion de documents scientifiques de niveau recherche, publiés ou non, émanant des établissements d'enseignement et de recherche français ou étrangers, des laboratoires publics ou privés.

1 Title: **Biogenic iron preserves structures during fossilization: A hypothesis**

2

3 Subtitle: Iron from decaying tissues may stabilize their morphology in the fossil record

4

5

6 Farid Saleh¹, Allison C. Daley², Bertrand Lefebvre¹, Bernard Pittet¹, and Jean Philippe

7

Perrillat¹

8

9

10 ¹Université de Lyon, Université Claude Bernard Lyon1, École Normale Supérieure de Lyon,
11 CNRS, UMR5276, LGL-TPE, Villeurbanne, France

12 ²Institute of Earth Sciences, University of Lausanne, Géopolis, CH-1015 Lausanne,
13 Switzerland

14

15

16 Corresponding author: Farid Saleh

17 Email: farid.saleh@univ-lyon1.fr

18 **Summary**

19 In this study, we hypothesize that iron from labile biological tissues, liberated during decay,
20 may have played a role in inhibiting loss of anatomical information during fossilization of
21 extinct organisms. Most tissues in the animal kingdom contain iron in different forms. The
22 most widely distributed iron-bearing molecule in modern taxa is ferritin, a globular protein
23 that contains iron crystallites in the form of ferrihydrite minerals. Iron concentrations in
24 ferritin are particularly high and ferrihydrites are extremely reactive. When organisms are
25 decaying on the sea floor under anoxic environmental conditions, ferrihydrites may initialize
26 the selective pyritization (replication in FeS_2) of some tissues. This model explains why some
27 decay-prone tissues are preserved, while other more resistant structures decayed and are
28 absent in many fossils. It also implies that structures described as brains in Cambrian
29 arthropods are not fossilization artifacts but instead a source of information on the anatomical
30 evolution at the dawn of complex animal life.

31

32 **Keywords:** exceptional fossil preservation, nervous systems, Burgess Shale, Fezouata Shale,
33 Chengjiang Biota, taphonomy, mineralization

34 **1. Introduction**

35 Inspecting the fossil record is crucial to understanding the biology of past life on earth.
36 Exceptionally preserved biotas, preserving soft-bodied metazoans (e.g. sponges; early
37 chordates) and their labile anatomies (e.g. digestive tracts, muscles, and nervous systems)
38 constitute a unique window on ancient ecosystems^[1-3]. For instance, the Burgess Shale
39 deposit in Canada yielded a considerable number of fossils shedding lights on spectacular
40 Cambrian taxa preserved in high fidelity^[4-10]. Exceptionally preserved soft parts in fossils
41 from the Fezouata Shale (Ordovician, Morocco) were decisive in ending long-standing
42 debates on the systematic affinities of various enigmatic taxa (e.g. machaeridians,
43 stylophorans)^[11-13]. The Chengjiang Biota (Cambrian, China) has also yielded a considerable
44 amount of soft arthropod taxa with complex nervous systems^[14-16]. In most cases, nervous
45 tissues from the Chengjiang Biota are pyritized (i.e. preserved in FeS₂) or show the
46 association of pyrite and organic matter^[14-17]. Pyritized tissues are frequently preserved alone
47 in the fossils, while other tissues or organs (except the cuticle or body walls) are completely
48 absent^[17]. Experimental taphonomic studies investigating how biological tissues decay under
49 various, controlled laboratory conditions questioned the validity of these paleontological
50 discoveries by showing that nervous systems have little to no chance of preservation because
51 they are observed to be rapidly lost under experimental conditions^[18-20]. These experimental
52 results have consequently given rise to contrasting conceptual frameworks in the paleontology
53 and evolutionary biology communities^[21-23]. Although vital to constrain preservation^[23],
54 experimental decay data should be interpreted carefully and not projected directly onto
55 enigmatic features in the geological record because fossils are not simply rotten carcasses and
56 decay resistance is an imperfect indicator of fossilization potential^[24]. Currently, there is no
57 model accounting for the preservation of a specific labile tissue in a specimen where other
58 more resistant tissues are completely absent. We investigate preservation patterns in such
59 problematic structures and compare it to the patterns of pyritization in non-altered sediments,
60 and propose an explanation for the contrast observed between the fossil record and modern
61 decay experiments.

62

63 **2. Enigmatic structures are preserved in pyrite and organic matter**

64 Anatomical structures described as brains in fossils from the Chengjiang Biota were
65 investigated using X-ray fluorescence mapping, which revealed the presence of carbon and
66 iron^[17] (Fig. 1a-d). Electron microscopy shows that iron occurs either as small euhedral
67 crystals (around 2 microns in size) or as framboids (around 10 microns in size)^[17] (Fig. 1e-h).
68 Pyrite crystal morphology indicates that pyritization occurred very early during the
69 fossilization process, shortly after the death of the organism^[25,26]. Carbon in these fossils is
70 preserved as compressed dark films^[17] (Fig. 1i, j). Chengjiang fossils broken through the
71 middle show pyrite overlaying carbonaceous films on both parts^[17], pointing to a centrifugal
72 pattern of pyritization (Fig. 1k). Centrifugal pyritization, similar to patterns of tissue
73 preservation in the Chengjiang Biota, is also present in fresh core sediments (Fig. 2a) from
74 levels with exceptional preservation within the Fezouata Shale, where Raman spectroscopy
75 identified large pyrite clusters surrounded by organic matter (Fig. 2b-d).

76 FeS₂ precipitation in sediments requires decaying organic material, and iron that is usually
77 provided by surrounding sediments in addition to sulfates SO₄⁻ from sea waters^[27,28]. Under
78 sulfate-reducing conditions, bacteria transform organic matter and sulfates into HS⁻ and then
79 to hydrogen sulfides H₂S, which react with Fe in a series of reactions to form pyrite^[26-28]. If
80 the sediment surrounding dead animals is poor in organic matter, as was the case in the
81 Fezouata Shale^[29], sulfate reduction is limited to decaying carcasses^[29]. Within a decaying
82 carcass, anatomical features can react differently to decay^[30]. Easily degradable structures
83 (e.g. tissues and organs formed of cells)^[3] constitute a hotspot for H₂S production, whereas

84 more resistant structures (e.g. biomineralized parts), do not produce enough H₂S, and thus do
85 not pyritize^[31]. Furthermore, decay discrepancies exist even between different fast decaying
86 cellular structures. Some cellular structures are solely degraded by external bacterial
87 communities, while others degrade under the activity of their internal microbial biota and
88 enzymes as well^[30,32]. If decay by external bacteria is dominant and iron is available,
89 pyritization starts at the outer part of the organic material where both H₂S and Fe are present,
90 leading to a centripetal pattern of preservation (Fig. 3a). This pattern is observed in the fossil
91 record^[27] and does not refute occurrences of centrifugal pyritization, because some tissues
92 decay under the activity of their internal bacteria and enzymes. If such internal decay is
93 dominant and iron is present, more H₂S is produced internally, leading to the centrifugal
94 pattern of preservation (Fig. 3b). It is likely that preserved structures in the Chengjiang Biota
95 and the Fezouata Shale decayed under the activity of their internal microbial biotas and
96 enzymes in the presence of iron. The proposed model based on H₂S limitation and production
97 patterns^[25,27,31] can explain (1) the centrifugal pyritization of nervous systems in Cambrian
98 arthropods and (2) the association of this anatomy to non-pyritized cuticular body walls that
99 did not produce enough H₂S for their pyritization^[25,31]. However, it fails to explain the
100 selective pyritization of a specific cellular structure (i.e. nervous system) while other internal
101 structures (e.g. digestive and vascular systems) decayed, producing H₂S, but did not pyritize.
102 Thus, it is crucial to investigate patterns of iron distribution in the sediment surrounding
103 decaying carcasses.

104

105 **3. Abiotic iron is not fast enough to preserve labile tissues**

106 The most classical and widely accepted sources of iron for pyritization are abiotic^[28,33]. In the
107 Fezouata Shale, iron oxides found in sediments (e.g. hematite α -Fe₂O₃; Fig. 2b-d) constitute
108 only a small fraction of the rock (i.e. <1%)^[26]. However, in a comparable way to numerous
109 Cambrian sites with exceptional fossil preservation, iron-rich silicates such as
110 berthierine/chamosite are dominant (i.e. between 5 and 15% of the total rock
111 composition)^[26,34]. Berthierine/chamosite results from the transformation of a primary clay
112 mineral (e.g. glauconite, odinite, kaolinite, or other similar precursor minerals)^[35] under
113 anoxic conditions and high iron concentrations^[26]. Thus, iron in this mineralogical phase
114 gives an estimate of the quantity of iron in the environment^[26,34,35]. The formation of
115 berthierine/chamosite in the Fezouata Shale required at least $\sim 8 \cdot 10^{-5}$ M (defined here the M
116 notation) of iron (see supplementary material). These concentrations are high and are slightly
117 less than the ones in modern anoxic sediments at 10^{-4} M and are enough to pyritize at the site
118 of decay^[27]. Thus, in theory and in terms of concentrations, abiotic iron is not a limiting
119 parameter in levels with exceptional preservation in the Fezouata Shale^[26] in a similar way to
120 sites with exceptional fossil preservation from the Cambrian^[34,36]. However, there must have
121 been other parameters controlling the availability of this iron during soft tissues degradation
122 and inhibiting pyrite from replicating all internal systems. Laboratory experiments have
123 shown that most anatomical structures in soft animals decay very fast within hours or days
124 after death^[18,20,37]. For instance, nervous tissues decayed under 11 days for chordates and
125 under 4 days for ecdysozoans^[18,20]. On the contrary, most iron-rich phases in contact with H₂S
126 require longer times to deliver their iron (Table 1)^[38]. This timing exceeds the timing of
127 biological tissue decay, especially for labile anatomies such as the brain^[18,20,32,37]. Thus,
128 another source of available iron must exist in order to selectively pyritize a tissue/organ
129 shortly after the death of the organism.

130

131 **4. Biogenic iron is available during decay**

132 If abiotic iron is not enough to start the pyritization process investigation on biogenic iron
133 source should take place. In analyzed samples (i.e. thin sections) from the Fezouata Shale,

134 maghemite (i.e. γ -Fe₂O₃ structurally similar to magnetite) is associated with pyrite (Fig. 2b-d).
135 Two widely recognized mechanisms for maghemite formation exist^[39,40]. In the first
136 mechanism, lepidocrocite, a fibrous iron oxide-hydroxide, transforms partially to maghemite
137 at temperatures around 200°C and completely at temperatures higher than 570°C^[39].
138 Maghemite can also result from buried ferrihydrites at temperatures between 100 and 300°
139 C^[40]. Sediments from the Fezouata Shale were cooked at temperatures between 100 and
140 200°C^[26,41]. These temperatures and the absence of lepidocrocite in the analyzed samples but
141 also from tens of other intervals in the Fezouata Shale^[26] indicate that maghemite in these
142 samples originates most probably from ferrihydrites. Ferrihydrite is a mineral with a wide
143 biological distribution that can explain why maghemite is only found in association with
144 pyritized organic matter and not in the sediment.

145 In all animals, ferritin is a metalloprotein that stores an excess of iron in the form of a hydrous
146 ferric oxide-phosphate mineral [FeO(OH)]₈ [FeO(H₂PO₄)] similar in structure to the mineral
147 ferrihydrite^[42,43]. Ferritin-ferrihydrites are found in nervous systems, muscles and sensory
148 organs such as the eyes^[44-46]. Ferritin is capable of storing as many as 4,500 iron atoms in its
149 core (i.e. concentration equivalent to 0.25M)^[46]. Increased accumulations of ferritin-
150 ferrihydrites were evidenced in marine invertebrates after their exposure to dysoxic/anoxic
151 conditions^[47] comparable to the environments in which animals from the Chengjiang Biota
152 and the Fezouata Shale were preserved^[48,49]. In experimental studies, it was shown that under
153 bacterial sulfate reducing (BSR) conditions and when sulfates are present, ferrihydrites
154 release high quantities (~ 87%) of reactive Fe^[50] (i.e. 0.22M). This iron delivery is 40%
155 higher than the yield from the same quantity of hematite^[50]. Furthermore, ferrihydrite is the
156 fastest to deliver reactive iron (Table 1), with a half-life under BSR conditions of only 2.8
157 hours^[38]. Ferrihydrite is also a solid phase meaning that it does not migrate^[51]. Thus, 0.11M
158 of iron becomes available *in-situ* within a couple of hours of the start of decay. These
159 concentrations are well above those in modern anoxic sediments^[27], and are definitely enough
160 to initiate pyritization at the site of decay.

161

162 **5. Biogenic iron explains the selective pyritization of soft anatomies**

163 Ferrihydrite in biological tissues constitutes a local source that rapidly provides high
164 quantities of reactive Fe^[38] that can initialize the process of pyritization. In this sense, shortly
165 after the death of an organism, decay of the most labile tissue starts producing H₂S. If this
166 tissue contains ferrihydrites, it produces as well a considerable amount of reactive iron (Fig.
167 4). The produced H₂S and Fe react to form pyrite nuclei (Fig. 4) that further growth from H₂S
168 and Fe availability as decay occurs (Fig. 4). The extensive activity of decay leads also to the
169 degradation of more resistant tissues (Fig. 4). However, if these less labile tissues are iron
170 poor, they produce only H₂S without iron (Fig. 4). Thus, the replication of such tissue in
171 pyrite is not initiated, leading to a loss of the original morphology or even the complete
172 disappearance of the tissue/organ (Fig. 4). When abiotic iron becomes available, it can play a
173 role in pyrite growth in tissues that previously provided biogenic iron (Fig. 4). This
174 hypothesis shows how biogenic iron stabilizes the morphology of decay-prone anatomical
175 structures, before the less reactive iron phases become available.

176

177 **6. Hypothesis testing requires a multidisciplinary approach**

178 Although fossil mineralization is common in the geological record^[53-58], little work has been
179 done to investigate the role of tissue chemistry during the mineralization process. Recently, it
180 was suggested that the recurrent association of a particular mineralogical phase
181 fluorapatite, Fe-sulfides (pyrite, pyrrhotite)

182 with a specific tissue in La Voulte-sur-Rhône (Jurassic, France), (precise the nature of the
183 mineralogical phase ? the type of tissue? And/or organism? Age and context sedim) can be
184 due to differences in the original biochemical signal of the organic matter^[52].

185 crustacean fossils preserved within carbonate-rich concretions from the Jurassic Konservat-
186 Lagerstätte of La Voulte-sur-Rhône (Ardèche, France)

187 However, much work remains to be done to precise the fate and behavior of biogenic iron
188 during the taphonomic processes, and fully enlighten the black box of pyritization.

189

190 In order to test the hypothesis and determine the precise roles played by biogenic iron and
191 iron from sediments, several lines of investigation should be undertaken combining
192 geochemical, biological and experimental taphonomy approaches.

193

194

195 It would be ideal to start testing the hypothesis on nonweathered fossils. However, to our
196 knowledge, no pyritized fossils from completely fresh sediments are discovered yet. Until
197 then, yielding investigations on fresh pyrite, not particularly associated with any fossil can
198 also be helpful because pyrite formation requires organic matter, and different organic
199 materials reflect different original biochemical compositions.

200 >> these sentences are not clear for me...

201

202 Iron isotopic investigations on pyrite crystals from both the sediments and the pyritized fossils
203 would help to decipher the multiple iron-sources and their role in pyritization. If these
204 isotopic investigations were made at the nanoscale, they can inform on the source and
205 chronology of iron delivery from the initiation of pyrite precipitation to the subsequent pyrite
206 crystals growth.

207

208 What about sulfur isotopes?

209 Do you think minor elements (bio-related?) would be of interest?

210

211 Biological approaches are also very helpful in testing this biogenic iron hypothesis, for
212 example by making a comparison between iron concentrations in different modern animal
213 groups and those measured in pyritized tissues found in the fossil record. An even more
214 detailed approach would be to quantify iron in different kinds of tissues within the same
215 group. For instance, according to this hypothesis, if a specific group shows a higher
216 concentration of iron in a specific tissue, we would expect to find this particular structure
217 pyritized more often than the others in the geological record.

218 All these quantitative data will also help calibrate the new proposed model and understand its
219 feasibility in natural environments. Most importantly, future decay experiments should focus
220 not only on the general environmental conditions that lead to exceptional preservation, but
221 also on the chemical signature surrounding each tissue during its degradation independently
222 from the physical ability of this tissue to resist decay. These decay experiments should be
223 done in the presence of different sediment compositions and under different bacterial
224 communities to see if decaying carcasses act variously under different environmental
225 conditions. Once iron sources, iron quantities in biological tissues, decay behavior, in addition
226 to favorable sedimentological phases are discovered, pyrite precipitation from biological
227 tissues could be replicated in laboratory aquariums.

228

229

230

231 Further isotopic investigations along this lines of the data presented here should be
232 undertaken on pyrite crystals should to determine iron sources at different stages of the
233 mineralization process. Additionally, the possible role of a biogenic iron source in other
234 exceptionally preserved biotas could be explored in this context^[40]. For example, at the
235 Burgess Shale (Cambrian, Canada), nervous systems are preserved as carbonaceous
236 compressions without any pyrite^[41,42] since overall conditions were favorable for
237 phosphatization^[43]. Nevertheless, berthierine, an iron-rich mineral known to slow down
238 decay^[44], is found in all levels with exceptional preservation. Future studies should investigate
239 if this iron-rich mineral, also reported in hundreds of other intervals with exceptional
240 preservation around the world^[26], is preferentially associated to specific labile soft parts.
241 Biological approaches for hypothesis testing including quantitative iron-analysis of modern
242 tissues and animals using mass spectrometry to help calibrate the new proposed model.
243 Finally, future decay experiments should focus not only on the general environmental
244 conditions that lead to exceptional preservation, but also on the chemical signature
245 surrounding each tissue during its degradation independently from the physical ability of this
246 tissue to resist decay.

247
248
249
250
251

252 7. Conclusions and outlook

253 The present biogenic iron hypothesis helps us understand the sole presence of the most-labile
254 tissues in some specimens where other more decay-resistant soft parts are absent. It also
255 shows that pyritization starts very early during decay, preserving in high fidelity tissues that
256 are originally iron-rich, resolving the morphological accuracy of Cambrian arthropod brains.
257 Furthermore, it indicates that both decay experiments and paleontological descriptions are
258 complementary, not incompatible. It opens new avenues of research by highlighting the
259 importance of tissue chemistry during the fossilization process especially in the case of
260 nervous tissues that are preserved in carbonaceous compressions without any pyrite^[59-61].

261

262 Acknowledgments

263 Figure 1a-j is used with minor edits from Ma et al., *Preservational pathways of corresponding*
264 *brains of a Cambrian euarthropod*, *Current Biology*, Volume 25, Issue 22, p. 7, 2015, with
265 permission from Elsevier. This paper is a contribution to the TelluS-INTERRVIE project
266 ‘Géochimie d’un *Lagerstätte* de l’Ordovicien inférieur du Maroc’ (2019) funded by the INSU
267 (Institut National des Sciences de l’Univers, France), CNRS. This paper is also a contribution
268 to the International Geoscience Program (IGCP) Project 653 – The onset of the Great
269 Ordovician Biodiversification Event. The Raman facility in Lyon (France) is supported by the
270 INSU. ACD’s contribution is supported by Grant no. 205321_179084 from the Swiss
271 National Science Foundation. The authors thank Gilles Montagnac for assistance during
272 Raman spectroscopy analyses. We also thank Robert Raiswell, Christian Klug, and the
273 anonymous reviewers for their comments and remarks.

274

275 Conflict of interest

276 None

277

278 References

279 [1] P. Van Roy, P. J. Orr, J. P. Botting, L. A. Muir, J. Vinther, B. Lefebvre, K. El Hariri,
280 D. E. G. Briggs, *Nature* **2010**, *465*, 215.

- 281 [2] A. C. Daley, J. B. Antcliffé, H. B. Drage, S. Pates, *Proc. Natl. Acad. Sci.* **2018**, *115*,
282 5323.
- 283 [3] F. Saleh, J. B. Antcliffé, B. Lefebvre, B. Pittet, L. Laibl, F. Perez Peris, L. Lustrì, P.
284 Gueriau, A. C. Daley, *Earth Planet. Sci. Lett.* **2020**, *529*, DOI
285 10.1016/j.epsl.2019.115873.
- 286 [4] J. Moysiuk, M. R. Smith, J.-B. Caron, *Nature* **2017**, *541*, 394.
- 287 [5] J. Moysiuk, J. B. Caron, *Proc. R. Soc. B Biol. Sci.* **2019**, *286*, 20182314.
- 288 [6] K. Nanglu, J. B. Caron, *Curr. Biol.* **2018**, *28*, 319.
- 289 [7] A. C. Daley, G. E. Budd, J. B. Caron, G. D. Edgecombe, D. Collins, *Science (80-.)*.
290 **2009**, *323*, 1597.
- 291 [8] J. Vannier, J. Liu, R. Lerosey-Aubril, J. Vinther, A. C. Daley, *Nat. Commun.* **2014**, *5*,
292 1.
- 293 [9] M. R. Smith, J.-B. Caron, *Nature* **2010**, *465*, 469.
- 294 [10] T. P. Topper, L. C. Strotz, L. E. Holmer, Z. Zhang, N. N. Tait, J. B. Caron, *BMC Evol.*
295 *Biol.* **2015**, *15*, 42.
- 296 [11] J. Vinther, P. Van Roy, D. E. G. Briggs, *Nature* **2008**, *451*, 185.
- 297 [12] J. Vinther, L. Parry, D. E. G. Briggs, P. Van Roy, *Nature* **2017**, *542*, 471.
- 298 [13] B. Lefebvre, T. E. Guensburg, E. L. O. Martin, R. Mooi, E. Nardin, M. Nohejlová, F.
299 Saleh, K. Kouraïss, K. El Hariri, B. David, *Geobios* **2019**, *52*, DOI
300 10.1016/j.geobios.2018.11.001.
- 301 [14] G. Tanaka, X. Hou, X. Ma, G. D. Edgecombe, N. J. Strausfeld, *Nature* **2013**, *502*, 364.
- 302 [15] P. Cong, X. Ma, X. Hou, G. D. Edgecombe, N. J. Strausfeld, *Nature* **2014**, *513*, 538.
- 303 [16] X. Ma, X. Hou, G. D. Edgecombe, N. J. Strausfeld, *Nature* **2012**, *490*, 258.
- 304 [17] X. Ma, G. D. Edgecombe, X. Hou, T. Goral, N. J. Strausfeld, *Curr. Biol.* **2015**, *25*,
305 2969.
- 306 [18] R. S. Sansom, S. E. Gabbott, M. A. Purnell, *Nature* **2010**, *463*, 797.
- 307 [19] D. J. E. Murdock, S. E. Gabbott, G. Mayer, M. A. Purnell, *BMC Evol. Biol.* **2014**, *14*,
308 DOI 10.1186/s12862-014-0222-z.
- 309 [20] R. S. Sansom, *Sci. Rep.* **2016**, *6*, 1.
- 310 [21] J. Liu, M. Steiner, J. A. Dunlop, D. Shu, *Proc. R. Soc. B Biol. Sci.* **2018**, *285*, DOI
311 10.1098/rspb.2018.0051.
- 312 [22] F. Saleh, B. Lefebvre, A. W. Hunter, M. Nohejlová, *Micros. Today* **2020**, *28*, 2.
- 313 [23] M. A. Purnell, P. J. C. Donoghue, S. E. Gabbott, M. E. McNamara, D. J. E. Murdock,
314 R. S. Sansom, *Palaeontology* **2018**, *61*, 317.
- 315 [24] L. A. Parry, F. Smithwick, K. K. Nordén, E. T. Saitta, J. Lozano-Fernandez, A. R.
316 Tanner, J.-B. Caron, G. D. Edgecombe, D. E. G. Briggs, J. Vinther, *BioEssays* **2018**,
317 *40*, 1700167.
- 318 [25] S. E. Gabbott, H. Xian-guang, M. J. Norry, D. J. Siveter, *Geology* **2004**, *32*, 901.
- 319 [26] F. Saleh, B. Pittet, J. Perrillat, B. Lefebvre, *Geology* **2019**, *47*, 1.
- 320 [27] J. D. Schiffbauer, S. Xiao, Y. Cai, A. F. Wallace, H. Hua, J. Hunter, H. Xu, Y. Peng,
321 A. J. Kaufman, *Nat. Commun.* **2014**, *5*, 5754.
- 322 [28] R. Raiswell, K. Whaler, S. Dean, M. . Coleman, D. E. . Briggs, *Mar. Geol.* **1993**, *113*,
323 89.
- 324 [29] R. R. Gaines, D. E. G. Briggs, P. J. Orr, P. Van Roy, *Palaios* **2012**, *27*, 317.
- 325 [30] D. E. G. Briggs, A. J. Kear, *Paleobiology* **1993**, *19*, 107.
- 326 [31] Ú. C. Farrell, *Paleontol. Soc. Pap.* **2014**, *20*, 35.
- 327 [32] A. D. Butler, J. A. Cunningham, G. E. Budd, P. C. J. Donoghue, *Proc. R. Soc. B Biol.*
328 *Sci.* **2015**, *282*, 20150476.
- 329 [33] R. Raiswell, D. E. Canfield, R. A. Berner, *Chem. Geol.* **1994**, *111*, 101.
- 330 [34] R. P. Anderson, N. J. Tosca, R. R. Gaines, N. Mongiardino Koch, D. E. G. Briggs,

- 331 *Geology* **2018**, *46*, 347.
- 332 [35] D. Tang, X. Shi, G. Jiang, X. Zhou, Q. Shi, *Am. Mineral.* **2017**, *102*, 2317.
- 333 [36] E. A. Sperling, C. J. Wolock, A. S. Morgan, B. C. Gill, M. Kunzmann, G. P.
- 334 Halverson, F. A. Macdonald, A. H. Knoll, D. T. Johnston, *Nature* **2015**, *523*, 451.
- 335 [37] A. D. Hancy, J. B. Antcliffe, *Geobiology* **2020**.
- 336 [38] D. E. Canfield, R. Raiswell, S. Bottrell, *Am. J. Sci.* **1992**, *292*, 659.
- 337 [39] T. S. Gendler, V. P. Shcherbakov, M. J. Dekkers, A. K. Gapeev, S. K. Gribov, E.
- 338 McClelland, *Geophys. J. Int.* **2005**, *160*, 815.
- 339 [40] L. Mazzetti, P. J. Thistlethwaite, *J. Raman Spectrosc.* **2002**, *33*, 104.
- 340 [41] G. M. H. Ruiz, U. Helg, F. Negro, T. Adatte, M. Burkhard, *Swiss J. Geosci.* **2008**, *101*,
- 341 387.
- 342 [42] F. M. Michel, V. Barron, J. Torrent, M. P. Morales, C. J. Serna, J.-F. Boily, Q. Liu, A.
- 343 Ambrosini, A. C. Cismasu, G. E. Brown, *Proc. Natl. Acad. Sci.* **2010**, *107*, 2787.
- 344 [43] N. D. Chasteen, P. M. Harrison, *J. Struct. Biol.* **1999**, *126*, 182.
- 345 [44] K. Hoda, C. L. Bowlus, T. W. Chu, J. R. Gruen, *Emery Rimoin's Princ. Pract. Med.*
- 346 *Genet.* **2013**, *1*.
- 347 [45] E. M. Aldred, C. Buck, K. Vall, E. M. Aldred, C. Buck, K. Vall, *Pharmacology* **2009**,
- 348 331.
- 349 [46] D. Dunaief, A. Cwanger, J. L. Dunaief, *Handb. Nutr. Diet Eye* **2014**, 619.
- 350 [47] K. Larade, K. B. Storey, *J. Exp. Biol.* **2004**, *207*, 1353.
- 351 [48] F. Saleh, Y. Candela, D. A. T. Harper, M. Polechová, B. Pittet, B. Lefebvre, *Palaios*
- 352 **2018**, *33*, 535.
- 353 [49] E. L. O. Martin, B. Pittet, J.-C. Gutiérrez-Marco, J. Vannier, K. El Hariri, R. Lerosey-
- 354 Aubril, M. Masrour, H. Nowak, T. Servais, T. R. A. Vandenbroucke, P. Van Roy, R.
- 355 Vaucher, B. Lefebvre, *Gondwana Res.* **2016**, *34*, 274.
- 356 [50] Y.-L. Li, H. Vali, J. Yang, T. J. Phelps, C. L. Zhang, *Geomicrobiol. J.* **2006**, *23*, 103.
- 357 [51] S. Wang, L. Lei, D. Zhang, G. Zhang, R. Cao, X. Wang, J. Lin, Y. Jia, *J. Hazard.*
- 358 *Mater.* **2020**, *384*, 121365.
- 359 [52] C. Jauvion, S. Bernard, P. Gueriau, C. Mocuta, S. Pont, K. Benzerara, S. and
- 360 Charbonnier, *Palaeontology* **2019**, *1*.
- 361 [53] D. E. Briggs, S. H. Bottrell, R. and Raiswell, *Geology* **1991**, *19(12)*, 1221.
- 362 [54] T. A. Hegna, M. J. Martin, S. A. Darroch, *Geology* **2017**, *45*, 199.
- 363 [55] L. Frey, A. Pohle, M. Rücklin, C. Klug, *Lethaia* **2019**.
- 364 [56] J. Rust, A. Bergmann, C. Bartels, B. Schoenemann, S. Sedlmeier, G. Köhl, *Arthropod*
- 365 *Struct. Dev.* **2016**, *45*, 140.
- 366 [57] T. W. Kammer, C. Bartels, W. I. Ausich, *Lethaia* **2016**, *49*, 301.
- 367 [58] R. Raiswell, R. Newton, S. H. Bottrell, P. M. Coburn, D. E. Briggs, D. P. Bond, S. W.
- 368 Poulton, *Am. J. Sci.* **2008**, *308*, 105.
- 369 [59] J. Ortega-Hernández, R. Lerosey-Aubril, S. Pates, *Proc. R. Soc. B Biol. Sci.* **2019**, *286*,
- 370 20192370.
- 371 [60] J. Ortega-Hernández, *Curr. Biol.* **2015**, *25*, 1625.
- 372 [61] L. Parry, J.-B. Caron, *Sci. Adv.* **2019**, *5*, eaax5858.
- 373 [62] S. Das, M. J. Hendry, *Chem. Geol.* **2011**, *290*, 101.

374

375 **Figure captions**

376 **Figure 1.** Preservation of Cambrian brains in *Fuxanhuia protensa* from the Chengjiang Biota.

377 a) YKLP 15006 shows dark brown areas interpreted as nervous tissues under direct

378 illumination. b) Carbon distribution in the studied specimen. c) Iron distribution. d) Merged

379 iron and carbon signals show an almost perfect superposition between these two elements.

380 White arrows indicate the rare places where both elements do not co-occur. e-h) Iron is

381 preserved in small euhedral and framboidal pyrite. i, j) Minerals overlay dark compressed
382 carbonaceous material. The distribution of carbonaceous films under pyrite minerals in both
383 part and counter-part suggest a centrifugal pattern of pyritization (k).

384 **Figure 2.** Pyritization in the Fezouata Shale. Pyrite crystals marked by white arrows in fresh
385 core deposits (a) showing a centrifugal pattern of pyritization (b, c). Colored points in (b) and
386 (c) correspond to the spectra shown in (d). Iron oxide phase identification is based on Raman
387 peak indexation in natural samples^[62].

388

389 Label each peak with the value of the Raman shift in cm^{-1} , it is easier for the reader to
390 compare data.

391

392 For the hematite and maghemite, do you have signal in the 1000- 1600 cm^{-1} range for
393 comparasion with the other spectra??

394

395

396 **Figure 3.** Patterns of soft tissue decay. a) Soft parts decaying under the activity of external
397 bacteria lead to a centripetal pyritization. b) Soft parts decaying under their own bacterial
398 community and enzymes contribute in a centrifugal pyritization.

399 **Figure 4.** Hypothesis for labile tissue preservation and resistant tissue loss.

400

Iron phase	Half-life
Goethite	11.5 days
Hematite	31 days
Magnetite	105 years
Reactive silicates	230 years
Sheet silicates	84000 years
Augite, amphibole	>84000 years

401 Table 1. Half-lives of iron phases under permissive conditions for pyrite precipitation.
402 (references ?) – what do you mean for “reactive” silicates?

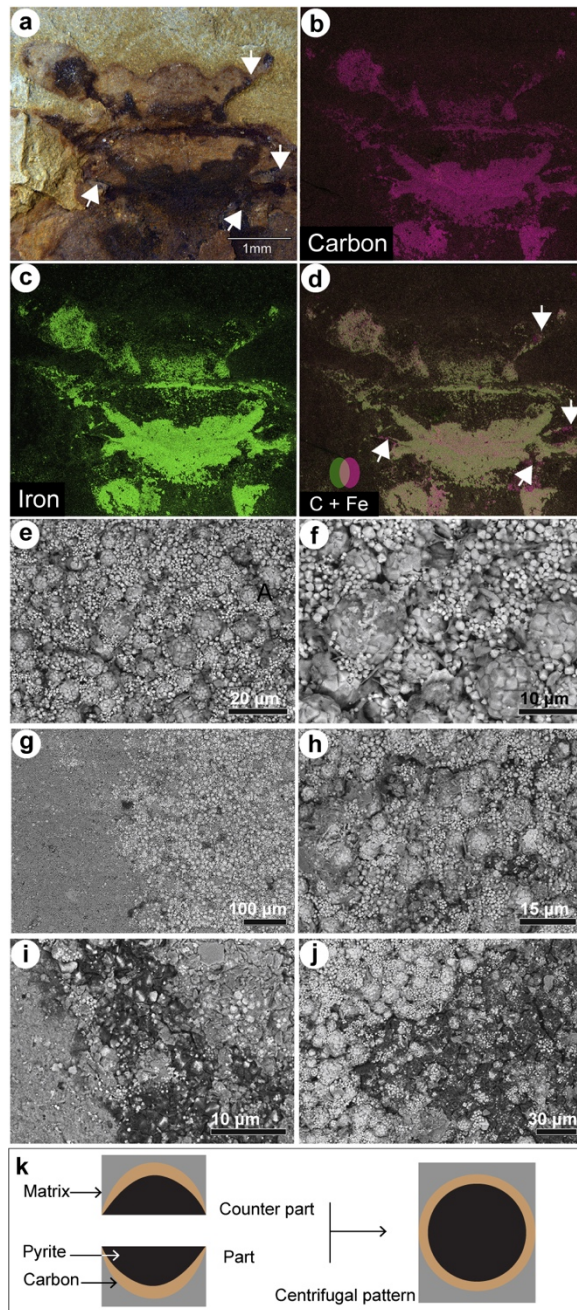


Figure 1

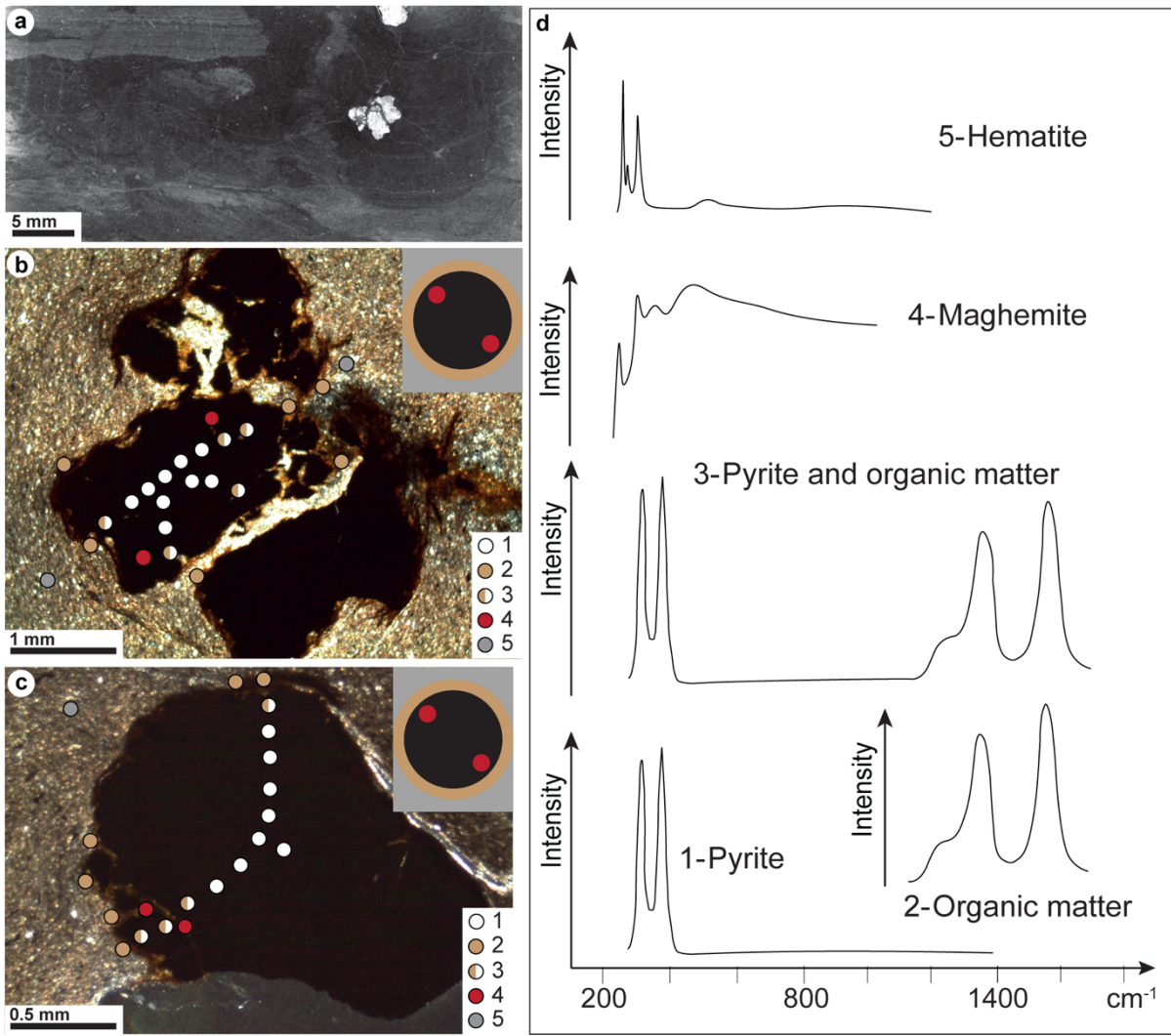


Figure 2

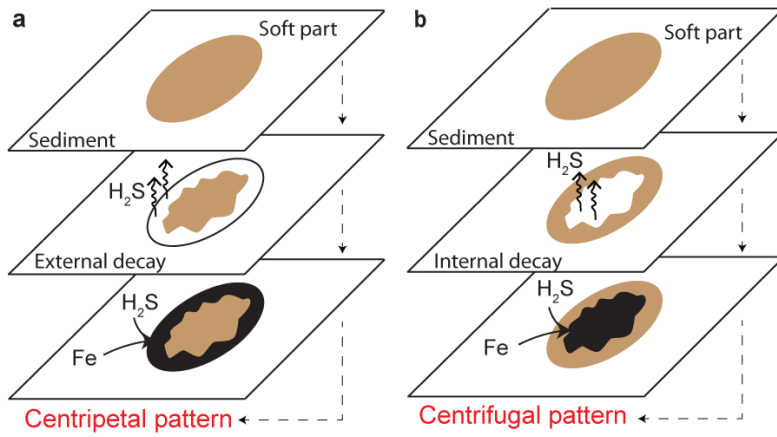


Figure 3

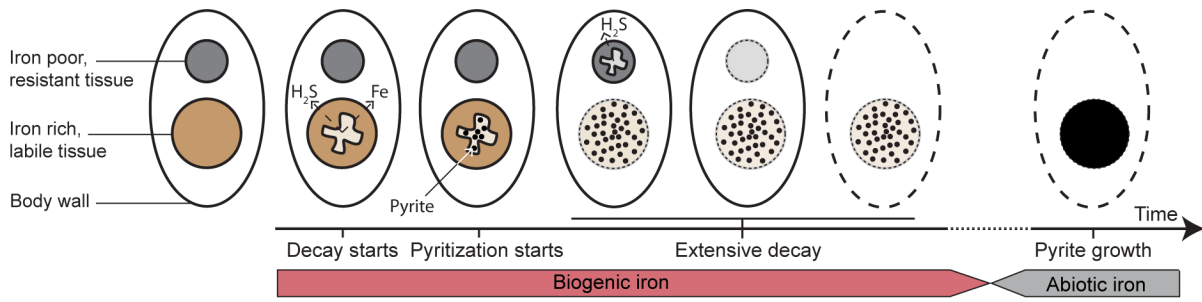


Figure 4